

ELECTRONIC SUPPLEMENTARY INFORMATION

Authors' Names and Affiliations

Liping Hou,^{†,‡} Meifang Guo,[‡] Jinliang Qiao,^{†,‡} and Eric T. Hsieh^{*‡}

[†]College of Materials Science and Engineering, Beijing University of Chemical
Technology, 100029, Beijing, People's Republic of China

[‡]Beijing Research Institute of Chemical Industry, SINOPEC, 100013, Beijing, People's
Republic of China

Title of the Primary Article

Re-assessing Melt versus Solution ¹³C NMR Spectral Sensitivity on Polyethylene

Table of Contents

SI-1. Molecular characteristics of PE sample material Marlex[®] resin EHM 6007 (Lot
No. 6390004)

Figure S-1: GPC Chromatogram of PE sample EHM 6007

Figure S-2: Full Solution ¹³C NMR spectrum of sample EHM 6007

Table S-1: Peak Assignments of PE Sample EHM 6007

SI-2. Guidelines for selecting baseline regions for a given peak

Figure S-3: Stacked spectra of the $\beta\delta^+$ peak region of Solution and Melt
experiments (7 days acquisition)

SI-3. OSW Calculations

Table S-2. Melt ¹³C NMR Observable PE Sample Weight Analysis

- Table S-3. Solution ^{13}C NMR Observable PE Sample Weight Analysis
- SI-4. NOE Considerations
- Figure S-4. Ratios of absolute u ($\delta^+\delta^+$) values (a) of Melt w/NOE over wo/NOE and (b) amongst three Solution experiments
- SI-5. Overall u ($\delta^+\delta^+$) profiles in absolute intensity mode
- Figure S-5. (a) Melt and (b) Solution u ($\delta^+\delta^+$) integrals in absolute intensity mode
- SI-6. Illustration of IW effect on σ ($\delta^+\delta^+$)
- Figures S-6. (a) u ($\delta^+\delta^+$), (b) σ ($\delta^+\delta^+$), and (c) **SNR** ($\delta^+\delta^+$) of the 15% Solution with **IW** at 3.0 and 1.9 ppm
- SI-7. Detection Limit (DL) comparisons between Solution and Melt for CH, $\alpha\delta^+$, and $\beta\delta^+$ peaks
- Figure S-7. DL comparison of the three Solution experiments for the CH (LCB) peak
- Figure S-8. DL comparison between Solution and Melt for the combined $\alpha\delta^+$ peaks
- Figure S-9. DL comparison between Solution and Melt for the combined $\beta\delta^+$ peaks

SI-1. Molecular characteristics of PE sample material Marlex[®] resin EHM 6007 (Lot No. 6390004)

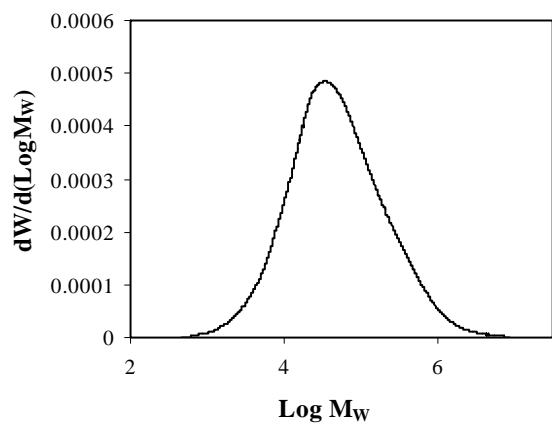


Figure S-1. Molecular Weight Distribution (MWD) of sample EHM 6007; 141.7K weight-average MW (M_w) and 18.8K number-average MW (M_n)

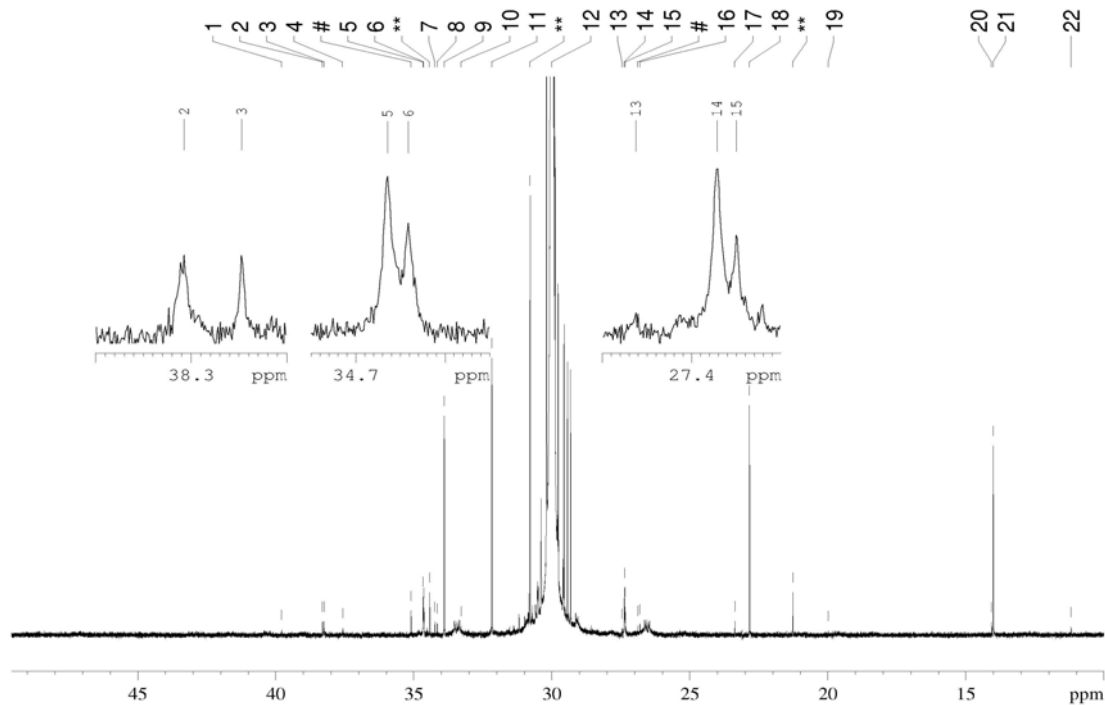


Figure S-2. Full Solution ¹³C NMR spectrum of sample EHM 6007

Table S-1. Peak Assignments of PE Sample EHM 6007

	<i>Peak chemical shifts(ppm)</i>	<i>Structural assignments</i>		<i>Peak chemical shifts(ppm)</i>	<i>Structural assignments</i>
1	39.778	CH(EBE)	12	30.000	$\delta^+ \delta^+$ (EE/EEE)
2	38.301	CH(LCB)	13	27.461	$\beta \delta^{\square+}$ (EPEE)
3	38.237	CH(EHE)	14	27.367	$\beta \delta^{\square}$ (LCB)/ \square $\beta \delta^+$ (EBEE)
4	37.573	$\alpha \delta^{\square+}$ (EPEE)	15	27.345	$\beta \delta^{\square+}$ (EHEE)
5	34.656	$\alpha \delta^{\square+}$ (LCB)	16	26.800	2B(EBE)
6	34.632	$\alpha \delta^{\square}$ (EHEE)	17	23.372	2B(EHE)
7	34.231	4B(EHE)	18	22.844	2S
8	34.146	$\alpha \delta^{\square}$ (EBEE)	19	19.986	1B(EPE)
9	33.902	Allylic carbon	20	14.077	1B(EHE)
10	33.284	CH(EPE)	21	14.016	1S
11	32.177	3S	21	11.188	1B(EBE)

Unknown Peak

** Peak of antioxidant BHT

SI-2. Guidelines for selecting baseline regions for a given peak

Let u denote the measured intensity of a peak, and σ the absolute value of the net deviation from the true baseline of the spectral region covered by the peak. Then the statistically meaningful expression for the true peak intensity is $u \pm \sigma$. Since this segment of the spectral region is covered by the peak such that it is impossible to measure the baseline intensity of this spectral segment directly, we could only hope to get a good estimate of σ from baseline regions *that may bear very similar characteristics as the one*

directly under the peak coverage. The following is a set of guidelines on selecting baseline regions and on obtaining baseline integral on such selections for best meeting the above underlined statement.

1. There should be no apparent peaks (based on visual inspection) within the selected baseline regions to be integrated.
2. The selected baseline regions of a given peak should be as close to the corresponding peak as possible, and be positioned to best mimic the anticipated baseline deviation of the corresponding peak integral.
3. The integral width (**IW**) should be the same for both the peak and its corresponding baseline regions.

In practice, selecting 6 to 8 baseline regions for each peak of interest would be about right. (There are practical pro's and con's to choosing too many or too few baseline regions for any given peak.) And σ is the Root Mean Square (RMS) of these baseline integrals, using either N or (N-1) for averaging, where N is the number of baseline integrals taken for the peak.

Rule #3 is always to be observed. But there are occasions when Rules #1 and #2 may not be both satisfied at the same time. Take the $\beta\delta^+$ peaks for example, the stacked spectra of the $\beta\delta^+$ region are shown in Figure S-3. There is overlap, to a varying degree, between the $\beta\delta^+$ peaks and the foothill of the $\delta^+\delta^+$ peak in all five spectra. If we were to following Rule #2, the selected baseline regions for the $\beta\delta^+$ peaks would no doubt contain foothill peak intensity from the $\delta^+\delta^+$ peak, which is in contradiction to Rule #1. But, for meeting the primary baseline region requirement of "bearing very similar

characteristics as the baseline region directly under the peak coverage”, Rule #1 would be overlooked in favor of Rule #2.

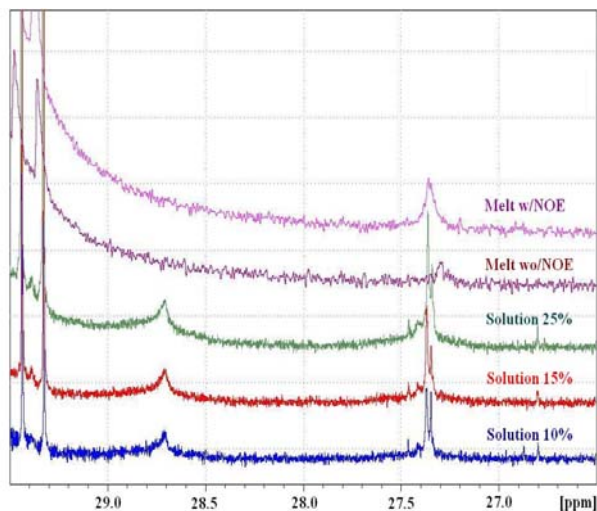


Figure S-3. Stacked spectra of the $\beta\delta^+$ region of Solution and Melt experiments (7 days acquisition)

SI-3. OSW Calculations

The actual **OSW** in each experiment can be accurately determined based on relevant dimensions of probe observe coil, rotor (in the case of Melt experiments) or sample tube (in the case of Solution experiments), along with theoretical and actually measured sample loading information. This information is detailed in Tables S-2 and S-3.

Table S-2. Melt ^{13}C NMR Observable PE Sample Weight Analysis

	<i>4mm</i>	<i>7 mm</i>
Rotor cavity inner height (cm)	1.70	1.65
Cap penetration depth (cm)	0.20	0.30
Effective rotor cavity depth (cm)	1.50	1.35
Rotor cavity ID (cm)	0.30	0.55
Maximum effective capacity (μl)	106.0	320.7
Maximum sample loading (mg)	94.4	285.5
Probe Observe Coil Height (cm)	0.95	0.95
Observable percentage (%)	63.3	70.4
Maximum observable quantity (mg)	59.8	200.9
Actually observed sample quantity (mg)		
Melt wo/NOE		141.1
Melt w/NOE		140.3

Table S-3. Solution ^{13}C NMR Observable PE Sample Weight Analysis

	<i>5 mm</i>	<i>10 mm</i>	<i>15 mm</i>
Tube ID (cm)	0.42	0.88	13.47
Observe Coil Height (cm)	1.6	2.4	3.0
Total observable volume (ml)	0.222	1.446	4.275
Observable sample quantity (mg)			
10% g/cc solution concentration	22.2	144.6	427.5
15% g/cc solution concentration	33.3	217.0	641.3
25% g/cc solution concentration	55.4	361.6	1069

A 7 mm rotor was used in our two Melt experiments. The calculated maximum capacity for this rotor was 320.7 μl . Using 0.89 g/cc to approximate PE melt density at 150 °C (the Melt NMR experiment temperature), we estimated the theoretical maximum melt sample loading of this rotor to be 285.5 mg. For better and safer laboratory practice,

our Melt experimental procedure called for packing the rotor with solid sample powder at room temperature before heating the sample to 150 °C inside the probe under mild spinning rate.²⁻⁴ At the end of each Melt experiment, the actual cooled sample weight was measured at 200.5 mg for the “no NOE” experiment and 199.4 mg for the “with NOE” experiment. Both were considerably less than the calculated maximum rotor loading capacity of 285.5 mg. The less-than-100% filling of the rotor was due primarily to the packing efficiency of the solid powder particles. When removed from the rotor, the cooled sample “plugs” were tubular in shape and hollow in the center, with reasonably uniform wall thickness from end to end. Each sample plug was measured at 1.35 cm in length, which is consistent with the rotor cavity dimensions. Since only 0.95 cm of the 1.35 cm total sample plug length was covered by the observe coil (corresponding to 70.37% of the amount of sample loaded), the actual observable sample weight of 141.1 mg for the wo/NOE experiment and 140.3 mg for the w/NOE experiment were easily derived.

A 10 mm probe was used for our three Solution experiments. The calculated and the actual observable sample weight should be the same when care is taken to keep the liquid level in the sample tube above the top of the observe coil coverage while spinning. Corresponding to sample solution concentrations of 10%, 15%, and 25% g/cc, the “observable sample weights” are calculated to be 144.6, 217.0, and 361.6 mg respectively. (See Table S-3 for details.) Also, these numbers are subject to minor variations due mainly to the achievable accuracy in measuring the solvent volume.

SI-4. NOE Considerations

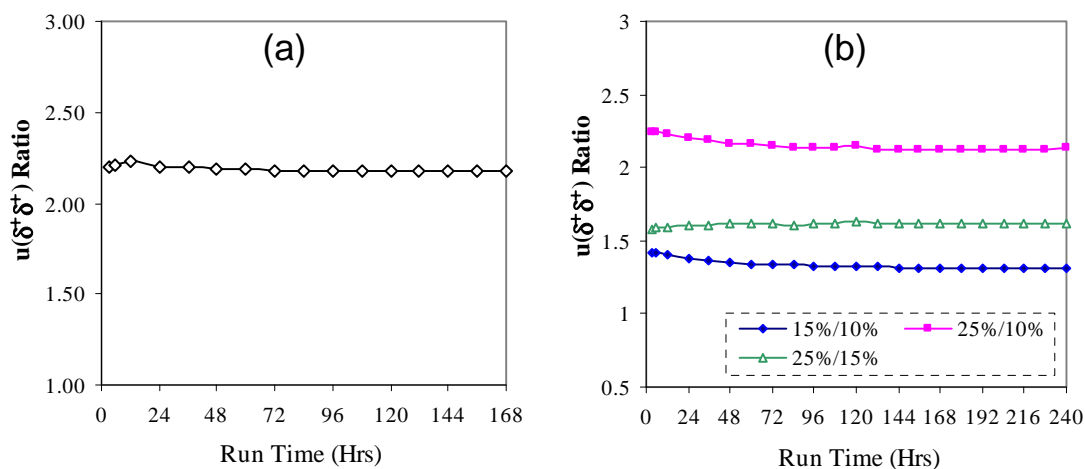
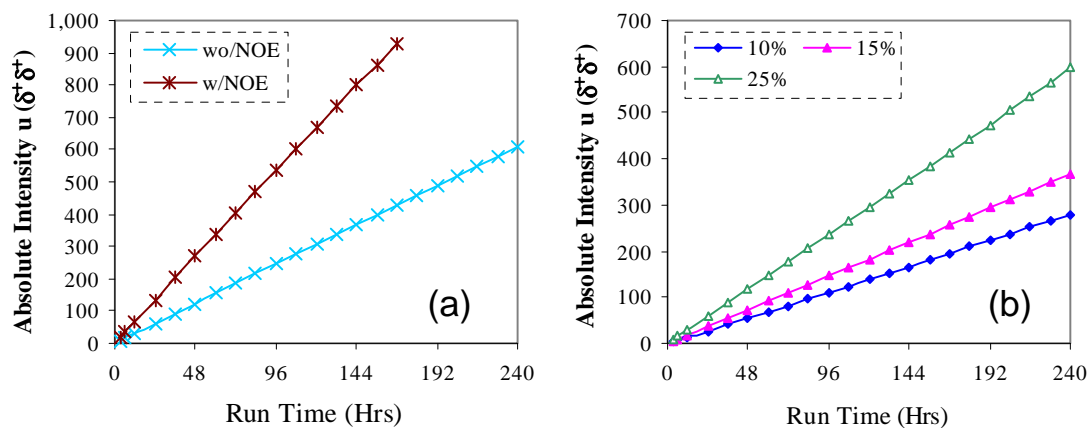


Figure S-4. Ratios of absolute $u(\delta^+\delta^+)$ values (a) of Melt w/NOE over wo/NOE and (b) amongst three Solution experiments

Shown in Figure S-4a are the ratios of Melt $u(\delta^+\delta^+)$, w/NOE over wo/NOE, for run times of 3 hours to 7 days. Melt w/NOE data with run times beyond 7 days were all corrupted due probably to an overloaded proton pulse amplifier. These ratio values are consistently at around 2.2 instead of 3. This is probably due, at least in part, to the likely presence of transient NOE in the wo/NOE data. Therefore, we conclude that the actual Melt NOE was at least 2.2, and could be as high as 3.

Solution $u(\delta^+\delta^+)$ ratios for 15%/10%, 25%/10%, and 25%/15% are shown in Figure S-4b. The ratio values were consistently around 1.34, 2.15, and 1.61 respectively, corresponding to NOE's of 2.7 and 2.6 for the 15% and the 25% Solution experiments assuming full NOE for the 10% Solution. A plausible explanation for this discrepancy is the 3.125 KHz decoupling field strength was too low for achieving full NOE at 15% and 25% concentrations. No inverse-gated Waltz-16 decoupling experiment was attempted on the Solution samples due to the likely presence of transient NOE.

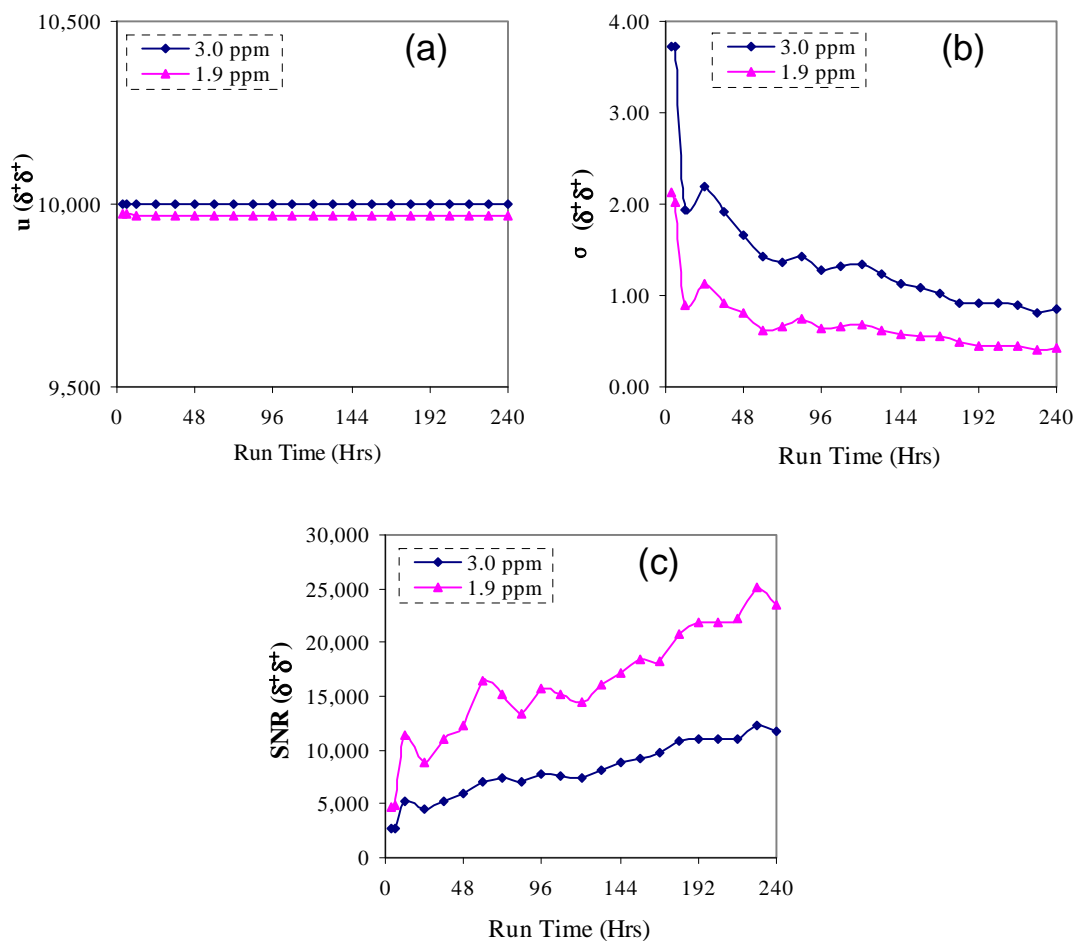
SI-5. Overall u ($\delta^+\delta^+$) profiles in absolute intensity mode



Figures S-5. (a) Melt and (b) Solution u ($\delta^+\delta^+$) integrals in absolute intensity mode

SI-6. Illustration of IW effect on σ ($\delta^+\delta^+$)

For assessing σ ($\delta^+\delta^+$), 8 baseline regions were selected near the $\delta^+\delta^+$ peak, following the guidelines detailed in SI-2, for each spectrum from the 15% Solution data set. The “IW=1.9 ppm” baseline regions were all located within the respective “IW=3.0 ppm” baseline regions (meaning the locations of the selected baseline regions were kept essentially the same). The resulting σ ($\delta^+\delta^+$) and SNR ($\delta^+\delta^+$) values were plotted in Figure S-6.



Figures S-6. (a) u ($\delta^+\delta^+$), (b) σ ($\delta^+\delta^+$), and (c) SNR ($\delta^+\delta^+$) of the 15% Solution with **IW** at 3.0 and 1.9 ppm

This magnitude of changes in SNR ($\delta^+\delta^+$) may appear alarming, or even suggesting the possibility of an artifact. Yet, when expressed using the “ $u \pm \sigma$ ” expression, the same outcome (using u and σ values at 3-hour run time for example) became $10,000 \pm 3.71$ (**IW**=3.0 ppm) and $9,971 \pm 2.12$ (**IW**=1.9 ppm) respectively. And all looked reasonable. A fair question to raise here is “what might have caused σ to increase with widening **IW**”. Intuitively the answer should lie with whatever baseline deviation contributing elements that would *accumulate through the process of integration*.

Therefore, true “noise” should not be such a factor since it tends to diminish upon addition due to its pure random nature. Other common baseline defects such as baseline sloping, baseline curvature, presence of unseen unknown peaks, contaminations from known yet unavoidable foothill of neighboring broad, and/or large peaks, among other things, are the more likely candidates. We had noticed changes in σ upon minor spectral phasing adjustments. Many of these “cumulative” contributing elements are location dependent. That was one of the reasons for suggesting “the baseline regions of a peak to be taken as close to that peak” in SI-2.

SI-7. Detection Limit (DL) comparisons between Solution and Melt for CH, $\alpha\delta^+$, and $\beta\delta^+$ peaks

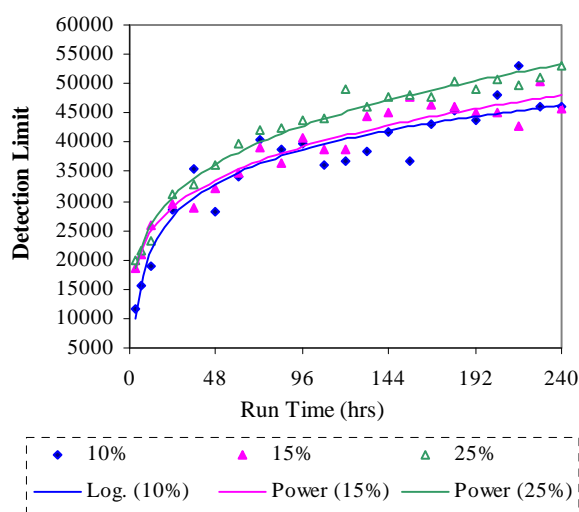


Figure S-7. DL comparison of the three Solution experiments for the CH (LCB) peak

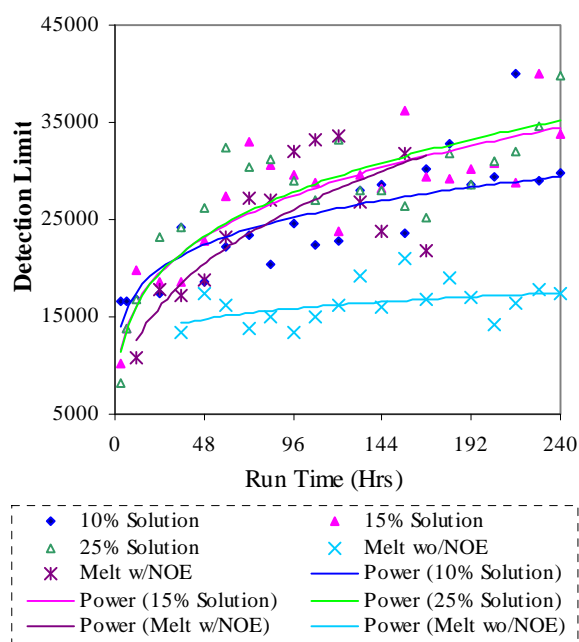


Figure S-8. DL comparison between Solution and Melt for the combined $\alpha\delta^+$ peaks

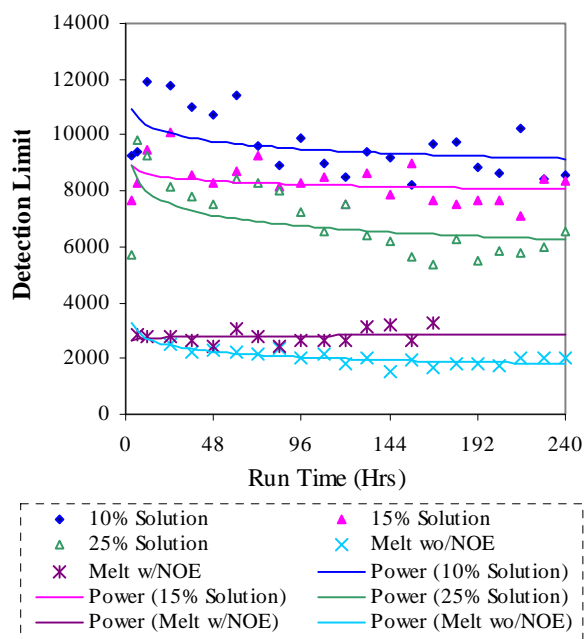


Figure S-9. DL comparison between Solution and Melt for the combined $\beta\delta^+$ peaks